Robust Performance Verification of IDCARC Controller for Hard Disk Drives

H. D. Taghirad, *Member, IEEE,* and E. Jamei

***Abstract*— Adaptive robust controller (ARC) has been recently developed for read/write head embedded control systems of hard disk drives (HDD). This structure is applicable to both track seeking and track following modes, and it makes the mode switching control algorithms found in conventional HDD servo system unnecessary. An Improved Desired Compensation ARC (IDCARC) scheme is proposed in this paper, in which traditional ARC is powered by a dynamic adaptive term. In this approach the adaptation regressor is calculated using reference trajectory information. Moreover, a robust analysis of this method is forwarded, in which a controller designed based on a simple model of system is verified in closed loop performance of a more comprehensive model of the system. Simulation result verifies the significant improvement of the performance of IDCARC compared to that of ARC and its robustness for this model. It is observed that in the presence of large disturbances the proposed method preserves stability and performance while the ARC fails even in stability.**

***Index Terms*— Adaptive robust control, hard disk drive, dynamic adaptation, robustness verification, nonlinear robust.**

I. INTRODUCTION

HARD Hard disk servo systems play a vital role for meeting the demand of increasingly high density and high performance hard disk drives. The servo system must achieve precise positioning of the read/write head on a desired track, called track following, and fast transition from one track to another target track called track seeking. The seeking time, should be minimized for faster data transmission rates. Because of the different control objectives in seeking and following modes, many drives use mode switching control (MSC) to accomplish both tasks. In MSC nonlinear controller routines such as proximate time optimal servo (PTOS) are popular choices for track seeking [1]. For track following, adaptive control [2,3], repetitive control, and many other approaches have been developed [4-10]. Switching of control mode from track seeking to track following should be so smooth that residual vibration of the suspension is minimal [4]. There are several attempts to develop unifying control algorithms, which work for both track seeking and following. Such control algorithms utilize the two degree-of-freedom control structure [4-6], composite nonlinear feedback control [7], gradient based track following [8], or other robust approaches for control [9,10]. Tomizuka and Yi proposed a 2DOF adaptive robust controller for HDD, [6], in which track seeking is accomplished by using a feed-forward controller based on offline identification. Yao proposed another ARC method for cancellation of the pivot nonlinearity and hysteresis effect in following mode [2]. Yao and Xu proposed Desired Compensation ARC (DCARC) for linear motors [11], in which the adaptation regressor is calculated using trajectory information based on Sadegh and Horowitz previous works [12]. The authors have proposed earlier an Improved DCARC, which includes dynamic adaptation mechanism to achieve hard disk performance necessities, such as fast disturbance attenuation and accuracy [13].

In this Paper this unifying controller structure is described based on Improved Desired Compensation ARC, and its closed loop performance is verified in present of high frequency resonant modes in the model. IDCARC combines DCARC advantages [11], in addition to faster disturbance attenuation, which is obtained through a dynamic adaptation routine included in the structure [6]. The algorithm is easily implementable as a unified embedded controller on both seeking and following modes. Reference trajectory is generated based on structural vibration minimized acceleration (SMART), in which the residual vibration of the suspension is minimal [4]. Hence, reference trajectory and its second order derivation, which is necessary in this ARC method, is generated online, and the differentiation from reference input becomes unnecessary. Moreover, as it is elaborated in Appendix I, the reference input signals based on SMART strategy will prevent saturation. The proposed new ARC controller has important advantages such as separating robust control design from parameter adaptation process [12], reducing the effect of measurement noise on the tracking, making adaptation process faster, and reducing the need for feed forward control in seeking time. The controller also takes into account the delay in seeking time, the model uncertainties and the effect of pivot friction. In order to fulfill high performance requirements, the model considered in controller performance verification, includes most significant nonlinear effect, namely the friction and high frequency resonant, hence the simulation results applied on this model is promising to work well in practice.

In the proceeding section, the plant modeling and problem formulation is introduced. In section III adaptive robust algorithm, DCARC and the proposed IDCARC has been introduced and its robust stability is analyzed, and finally, the comparative studies are elaborated in section IV.

II. PROBLEM FORMULATION AND DYNAMICAL MODELS

A comprehensive mathematical model of the hard disk servo drive system is given as following [1, 9]:

$$\begin{cases} \dot{x}_1 = x_2 \\ J\dot{x}_2 = u - Bx_2 - A_f Sign(\dot{y}) - F_{hys} + F_{hi} + F_d \\ y = x_1 \end{cases} \quad (1)$$

in which, $x = [x_1, x_2]^T$ represent the state vector of the angular position and velocity, y is the position, J is the moment of inertia, u is the control input, B and A_f are coefficient of viscous and coulomb friction, respectively, F_{hys} and F_{hi} represent the effect of hysteresis loop and high frequencies uncertainties, respectively, and, F_d is the external disturbance. Let y_r be the reference motion trajectory. The control objective is to synthesize a control input u such that the output y tracks $y_r(t)$ as close as possible, despite various model uncertainties.

Fig. 1 shows different components of HDD, and the parameters used in the simulations are given in Table I. A simpler version of the model, in which the hysteresis, high frequency resonant, and the external disturbances are considered as an uncertain disturbance is

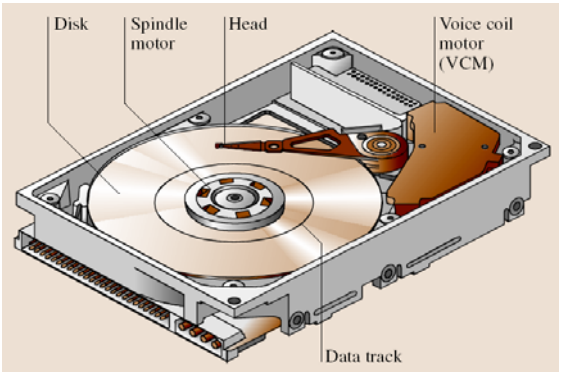

Fig. 1. Hard disk drive components

assumed to be the basis of the adaptive robust controller design. However, for robustness verification of the closed loop performance a more comprehensive model including high frequency resonance modes [1], are used. The transfer function of the more comprehensive system is derived from identification experiments, and its frequency response is illustrated in Fig. 2. The model is identified using least-squares estimation on the frequency response. The identified transfer function is a tenth order non-minimum phase system, with two real poles, one of them right at the origin and another one close to the origin, which resembles a the dynamical behavior reported in [9]. The identified poles are: $10^4\times(0,$ -0.0012, $-0.0283\pm5.6548i$, $-0.1257\pm2.510i$, $-0.0069\pm1.3823i$, $-0.0022\pm0.0439i$). Moreover, the zeros are located at: $10^5\times$ ($-6.8070, 0.0017\pm0.4360i$, $-0.0008\pm0.1394i$, $-0.0002\pm0.0044i$).

In Fig. 2, the frequency response of the simple model (dash dot) is compared to that of more comprehensive model (solid). The input to the system is the VCM current measured in (mA) and the output of the system is the head position in (mm). As it is seen in Fig. 2 the more comprehensive model contains a resonance frequency about 2200 Hz. The consistency of the simplified model to the more comprehensive model is clearly illustrated by the perfect fit at low frequencies. The controller design goal is to obtain desired tracking performance and to avoid exciting high frequency modes especially during following mode.

III. Adaptive Robust Control

In order to design the Adaptive robust controller, identification of a simple model for the system is sufficient. The state space representation of this model can be linearly parameterized as:

$$\dot{x}_1 = x_2 \tag{2}$$

$$\theta_1\dot{x}_2 = u - \theta_2 x_2 - \theta_3 Sign(x_2) + \theta_4 + \tilde{d} \tag{3}$$

In which $\theta_4 = d_n$ is the nominal value of the lumped disturbance d .

TABLE I
Parameter of Hard Disk Drive Components

Description	Symbols	Quantity
Spindle speed	ω	3623 rpm
Track pitch	L_{track}	$1\mu m$
Coil resistance and Current sensing resistance	R	8.516 Ω
Viscous Friction	B	2.54 $N-\sec/m$
Torque constant	K_T	20 N/A
Moment of inertia	I_b	$12.5\times10^{-6} kg\cdot m^2$

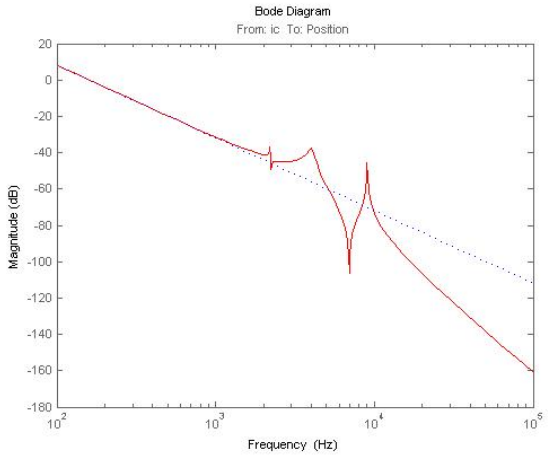

Fig. 2. Bode diagram of HDD ideal model (dashed) and more complete model (solid)

It is assumed that, all the effect of hysteresis and high frequency resonance is absorbed into the term d . In order to describe the controller structure, consider the following assumptions.

Assumptions: The following bounds and structures for uncertainties and disturbances are assumed.

$$\theta \in \Omega_\theta \equiv \{\theta : \theta_{\min} < \theta < \theta_{\max}\} \tag{4}$$

$$\tilde{d} \in \Omega_d \equiv \{\tilde{d} : |\tilde{d}| < \delta_d\} \tag{5}$$

In which, $\theta_{\min} = [\theta_{1\min},...,\theta_{4\min}]^T$, $\theta_{\max} = [\theta_{1\max},...,\theta_{4\max}]^T$ and δ_d are assumed to be known. Let $\hat{\theta}$ denotes the estimate of θ and $\tilde{\theta}$ the estimation error (i.e. $\tilde{\theta} = \hat{\theta} - \theta$). In view of (4) the following adaptation law with discontinuous projection modification can be used:

$$\dot{\hat{\theta}} = \Pr oj(\Gamma\tau) \tag{6}$$

where, $\Gamma > 0$ is a diagonal matrix, τ is adaptation function to be synthesized later. The projection mapping is defined as:

$$\Pr oj_{\hat{\theta}}(\bullet) = [\Pr oj_{\hat{\theta}_1}(\bullet_1),..., \Pr oj_{\hat{\theta}_p}(\bullet_p)]^T$$

$$\Pr oj_{\hat{\theta}_i}(\bullet_i) = \begin{cases} 0, (if\ \hat{\theta}_i = \theta_{i\max}\ \&\ \bullet_i > 0) or (if\ \hat{\theta}_i = \theta_{i\min}\ \&\ \bullet_i < 0) \\ \bullet_i \qquad Otherwise \end{cases} \tag{7}$$

It can be shown that for any adaptation function τ the projection mapping used in (7) guarantees [15]:

$$\begin{aligned} &P1 \qquad \hat{\theta} \in \Omega_\theta \equiv \{\hat{\theta} : \theta_{\min} \le \hat{\theta} \le \theta_{\max}\} \\ &P2 \qquad \tilde{\theta}^T(\Gamma^{-1}\Pr oj(\Gamma\tau) - \tau) \le 0 \qquad \forall\tau \end{aligned} \tag{8}$$

A. ARC Controller Design

Define a switching-function quantity as $p = \dot{e} + k_1 e = x_2 - x_{2eq}$, where $x_{2eq} \equiv \dot{y}_d - k_1 e$ and $e = y - y_d(t)$ is the output tracking error, $y_d(t)$ is the desired trajectory to be tracked by y , and k_1 is any positive feedback gain. With respect to (3) one can obtain:

$$J\dot{p} = u - \theta_1\dot{x}_{2eq} - \theta_2 x_2 - \theta_3 Sign(x_2) + \theta_4 + \tilde{d} = u + \varphi^T\theta + \tilde{d} \tag{9}$$

If p is small or converges to zero exponentially, then the output tracking error e , will be small or converges to zero exponentially. This is because $G_p(s) = e(s)/p(s) = 1/(s+k_1)$ is a stable transfer function. Hence, the rest of design is to make p as small as possible. Where $\varphi^T = [-\dot{x}_{2eq}, -x_2, -Sign(x_2), 1]$ and $\dot{x}_{2eq} = \ddot{y}_d - k_1\dot{e}$.

The control law consists of two parts:

$$u = u_a + u_s \qquad u_a = -\varphi^T\hat{\theta} \tag{10}$$

$u_s = u_{s1} + u_{s2} \qquad u_{s1} = -k_2 p$

Where u_a is the adjustable model compensation needed for achieving perfect tracking, and u_s is a robust control law consist of two parts: u_{s1} is used to stabilize the nominal system which is a proportional feedback in this case, and u_{s2} is a robust feedback term to attenuate the effect of model uncertainties, which will be synthesize later. Substituting (10) in to (9), and simplifying one can obtain:

$$J\dot{p} = u_s - \varphi^T \tilde{\theta} + \tilde{d} \tag{11}$$

Noting Assumption 1 and P1 of (8), there exist a u_{s2} such that the following two conditions are satisfied:

$$i)\, p\{u_{s2} - \varphi^T \tilde{\theta} + \tilde{d}\} \le \varepsilon \qquad ii)\, pu_{s2} \le 0 \tag{12}$$

where, ε is a design parameter which can be chosen arbitrarily small. From condition (i) u_{s2} is synthesized to dominate the model uncertainties coming from both parametric uncertainties $\tilde{\theta}$ and uncertain nonlinearities $\tilde{d}$, and condition (ii) guarantees that u_{s2} is dissipative in nature so that it does not interfere with the functionality of the adaptive control part u_a. If the adaptation function in (6) is chosen as $\tau = \varphi.p$ then the ARC control law in (10), whose general block diagram is depicted in Fig. 3, guarantees all signals to be bounded [11]. In addition, if after finite time t_0, there exist only parametric uncertainties i.e., ($\tilde{d} = 0, \forall t \ge t_0$), then zero final tracking error is achieved, i.e. $e \to 0$ and $p \to 0$ as $t \to \infty$.

B. *Improved Desired Compensation ARC*

In the ARC design presented, the regressor φ in the model compensation u_a (Eq. 10) and adaptation function $\tau = \varphi.p$ depends on the actual measurement of the velocity x_2. Thus the effect of measurement noise is severe. Moreover, in spite of condition ii of (12), there still exist certain interaction between the model compensation u_a and the robust control u_s. This may complicate controller gain tuning process in an experimental implementation. Sadegh and Horowitz [9] proposed a desired compensation adaptation law, in which the regressor is only calculated by desired trajectory information. The idea is then incorporated in the ARC design in some other works. However, as detailed in [13], DCARC alone cannot guarantee high accuracy and disturbance attenuation as a HDD controller. Here, we introduced Improved DCARC, in which dynamics is added to the adaptation law. In the IDCARC, the control law and the adaptation function have the same form as (10) and $\tau = \varphi.p$, respectively, however, regressor φ is substituted by the desired regressor φ_d:

$$u = u_a + u_s \qquad u_a = -\varphi_d^T \hat{\theta} \qquad \tau = \varphi_d\, p \tag{13}$$

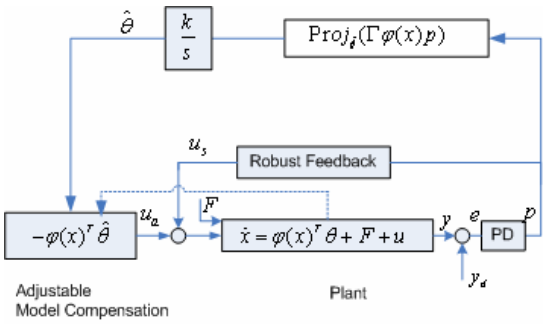

Fig. 3. ARC Block diagram

Where $\varphi_d^T = [-\ddot{y}_d, -\dot{y}_d, -Sign(\dot{y}_d), 1]$. Substituting (13) into (11) and noting that $x_2 = \dot{y}_d + \dot{e}$, one obtains:

$$J\dot{p} = u_s - \varphi_d^T \tilde{\theta} + \underline{(\theta_1 k_1 - \theta_2)\dot{e} + \theta_3[Sign(\dot{y}_d) - Sign(x_2)]} + \tilde{d} \tag{14}$$

Note that since only the desired trajectory information $y_d(t)$ is needed in this case, the effect of noise is reduced significantly. Comparing (14) with (11), it can be seen that two additional terms (under lined) has been appeared, which may demand a strengthened robust control function u_s for a robust performance. The strengthened robust control function u_s has the same form as (10):

$$u_s = u_{s_1} + u_{s_2} \qquad u_{s_1} = -k_{s_1} p \tag{15}$$

The drawback of using desired regressor φ_d instead of measured one φ, is the inability to attenuate disturbance fast enough to accommodate hard disk drives requirements. This is remedied in IDCARC by using a dynamical adaptation law. As depicted in Fig. 4 it is proposed to change the *I* (integrator) estimator with a *PI* (Proportional-Integral) routine in estimation mechanism of θ. To elaborate these changes consider the model of hard disk servo system in identification procedure.

$$\textit{Real system: } u + d = J\ddot{y} + B\dot{y} + A_f\, Sign(\dot{y}_d) \tag{16}$$

It is suggested to reach to:

$$\textit{Ideal system: } p = J\ddot{y}_d + B\dot{y}_d \tag{17}$$

Lemma 1: suppose; $y(t + t_d) = y_d(t)$ in which, t_d is the system time delay. Hence, for the generated signal $y(t + t_d) \ge y(t)$, and therefore:

$$y(t) = \alpha_1 y_d(t)\ \&\ \dot{y}(t) = \alpha_2 \dot{y}_d(t)\ \&\ \ddot{y}(t) = \alpha_3 \ddot{y}_d(t) \tag{18}$$

where α_1, α_2 and α_3 are constant coefficient depending on time. Without loss of generality assume $u_{s2} = 0$; hence, $u = u_a + p$ by substitution of (13) into (16) with respect to (18) and some simplifications we reach to:

$$p + \underline{(\hat{J} - J\alpha_3)\ddot{y}_d + (\hat{B} - B\alpha_2)\dot{y}_d + (\hat{A}_f\, Sign(\dot{y}_d) - A_f\, Sign(\alpha_2 \dot{y}_d))} + (d - \hat{d}) = 0 \tag{19}$$

Now we propose adding a dynamic term to u_a.

$$\begin{aligned} p + (\dot{\hat{J}}\ddot{y}_d + k\hat{J}\dddot{y}_d - J\alpha_3\ddot{y}_d) + (\dot{\hat{B}}\dot{y}_d + k\hat{B}\ddot{y}_d - B\alpha_2\dot{y}_d) + \\ (\dot{\hat{A}}_f\, Sign(\dot{y}_d) + k\hat{A}_f\, Sign(\dot{y}_d) - A_f\, Sign(\alpha_2\dot{y}_d)) \\ + (\dot{d} - \dot{\hat{d}} - k\hat{d}) = 0 \end{aligned} \tag{20}$$

Furthermore, each term inside the brackets consist of a first order differential equation, i.e. by this means a suitable dynamics is introduced for the compensation signal. Since, by the introduced dynamics, (16) approaches to (17) dynamically, hence better disturbance and friction compensation is obtained. Thus, the adaptation law can be interpreted as adding integrator proportional to u_a, as depicted in Fig. 4. The proposed improved IDCARC law and the adaptation function have the same from as (13), respectively, but with the difference that $\tau = \varphi_d \cdot p$ is subjected to the introduced dynamics of τ_d as:

$$u = u_a + u_s \qquad u_a = -\varphi_d^T \hat{\theta} \qquad \tau_d = \varphi_d(\dot{p} + kp) \tag{21}$$

Equations (13) to (18) can be applied with this improvement to IDCARC. One can write (14) as:

$$\dot{p} = u_s - \varphi_d^T(\tilde{\theta}) + \underline{(\theta_1 k_1 - \theta_2)\dot{e} + \theta_3[Sign(\dot{y}_d) - Sign(x_2)]} + \tilde{d} \tag{22}$$

Where $\tilde{\theta} = (\hat{\theta} + k\dot{\hat{\theta}}) - \theta$. Applying mean value theorem, we have;

$$Sign(x_2) - Sign(\dot{y}_d) = g(x_2, t)\dot{e} \tag{23}$$

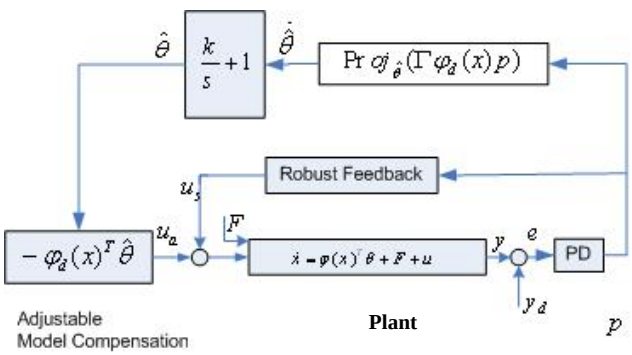

Fig. 4. IDCARC Block diagram

In which, $g(x_2,t)$ is a nonlinear function. The strengthened robust control function u_s has the same form as (10):

$$u_s = u_{s1} + u_{s2} \qquad u_{s1} = -k_{s1} p \tag{24}$$

but with k_{s1} being a nonlinear function. We must have $k_{s1} \geq k_2 + \theta_1 k_1 - \theta_2 - \theta_3 g + (\theta_2 + \theta_3 g)^2 / 2\theta_1 k_1$ such that the matrix A defined below becomes positive definite.

$$A = \begin{bmatrix} k_{s1} - k_2 - \theta_1 k_1 + \theta_2 + \theta_3 g & -\frac{1}{2} k_1 (\theta_2 + \theta_3 g) \\ -\frac{1}{2} k_1 (\theta_2 + \theta_3 g) & \frac{1}{2} J k_1^3 \end{bmatrix} \tag{25}$$

u_{s2} required to satisfy following constrains similar to (12).

$$\begin{aligned} &i) \quad p\{u_{s2} - \varphi_d^T \tilde{\theta} + \tilde{d}\} \leq \varepsilon \\ &ii) \quad p u_{s2} \leq 0 \end{aligned} \tag{26}$$

As shown in Fig. 5 Because of additional term in (22) the robust term of IDCARC u_s in (24) must be stronger than robust term of ARC, whereas better adaptation mechanism in IDCARC causes lower upper bounds for $p^2(t)$ in IDCARC, simulations confirm this general observation.

Theorem 1: If the IDCARC law (14) is applied, then

A) In General, all signals are bounded. Furthermore, the positive definite function

$$V_s = 1/2 J p^2 + 1/2 J k_1^2 e^2 \tag{27}$$

is bounded by:

$$V_s \leq \exp(-\lambda t) V_s(0) + \frac{\varepsilon}{\lambda}[1 - \exp(-\lambda t)] \tag{28}$$

where $\lambda = \min\{2k_2 / \theta_{1\max}, k_1\}$.

B) If after finite time t_0 **,** there exist parametric uncertainties only (i.e., $\tilde{d} = 0, \forall t \geq t$) then, in addition to result in (A), zero final tracking error is also achieved, i.e.:

$$e \to 0 \quad and \quad p \to 0 \quad as \quad t \to \infty .$$

Proof: Along the trajectory of (20), the time derivative of V_s given by (27) is:

$$\begin{aligned} \dot{V_s} &= p\{u_s - \varphi_d^T \tilde{\theta} + (\theta_1 k_1 - \theta_2)\dot{e} \\ &\quad + \theta_3 [S_f(\dot{y}_d) - S_f(x_2)] + \tilde{d}\} + J k_1^2 e \dot{e} \end{aligned} \tag{29}$$

Applying (23) and (24) where as $\dot{e} = p - k_1 e$ and $\theta_1 = J$, we have:

$$\begin{aligned} \dot{V}_s &\leq p\{u_{s2} - \varphi_d^T \tilde{\theta} + \tilde{d}\} + (-k_{s1} + \theta_1 k_1 - \theta_2 - \theta_3 g) p^2 \\ &\quad + k_1 (\theta_2 + \theta_3 g) e p - J k_1^3 e^2 \end{aligned} \tag{30}$$

If A given by (25) is positive definite, then

$$\dot{V}_s \leq p\{u_{s2} - \varphi_d^T \tilde{\theta} + \tilde{d}\} + k_2 p^2 - \frac{1}{2} J k_1^3 e^2 \tag{31}$$

With condition (26-i) and $\lambda = \min\{2k_2 / \theta_{1\max}, k_1\}$, the derivative of V_s becomes:

$$\dot{V}_s \leq -\lambda V_s + \varepsilon \tag{32}$$

Which leads to (28) and the results in A) is proved. Now consider a situation on B) where $\tilde{d} = 0$, $\forall t \geq t_0$. Choose a positive definite function V_a as:

$$V_a = V_s + \frac{1}{2} \tilde{\theta}^T \Gamma^{-1} \tilde{\theta} \tag{33}$$

From (30), condition ii) of (26), and P2 of (8), the derivative of V_a satisfies:

$$\dot{V}_a \leq -k_2 p^2 - \frac{1}{2} J k_1^3 e^2 + \tilde{\theta}^T \Gamma^{-1} (\dot{\hat{\theta}} - \Gamma \tau) \leq W \tag{34}$$

Where $W = -k_2 p^2 - \frac{1}{2} J k_1^3 e^2$. Therefore, $W \in L_1$ and $V_a \in L_\infty$. Since all signal are bounded, and it is easy to check $\dot{W}$ is bounded and thus uniformly continuous. By Barbalet's lemma $W \to 0$ as $t \to 0$. ■

Remark: Let h be any smooth function satisfying: $h \geq \|\theta_M\| \, \|\varphi\| + \delta_d$ where $\theta_M = \theta_{\max} - \theta_{\min}$ .Then, one smooth example of u_{s2} satisfying (12) is given by: $u_{s2} = -\frac{1}{4\varepsilon} h^2 p$, also for (26): $h' \geq \|\theta_M\| \, \|\varphi_d\| + \delta_d$, $u_{s2} = -\frac{1}{4\varepsilon} h'^2 p$.

IV. Comparative Studies

A. Performance Indices

Simulations studies have been performed for ARC, DCARC, and IDCARC to verify the effectiveness of the proposed controller in terms of tracking errors, and disturbance rejection. In order to compare simulation results for representatives of different controllers proposed for such system as in literature [4, 6, 7], the following performance indices are used.

I1) $L_2[e] = \sqrt{\frac{1}{T_f} \int_0^{T_f} |e|^2 dt}$ is an average tracking performance index, for the entire error curve $e(t)$. T_f represents the total simulation time in here.

I2) $e_M = \max_t \{|e(t)|\}$, is the maximum absolute value of the tracking error.

I3) $e_F = \max_{T_f - 1 \leq t \leq T_f} \{|e(t)|\}$, is the maximum absolute value of the tracking error during the last one millisecond.

I4) $L_2[u] = \sqrt{\frac{1}{T_f} \int_0^{T_f} |u|^2 dt}$, is the mean of the control input.

I5) $c_u = L_2[\Delta u] / L_2[u]$, is the control input chattering, where

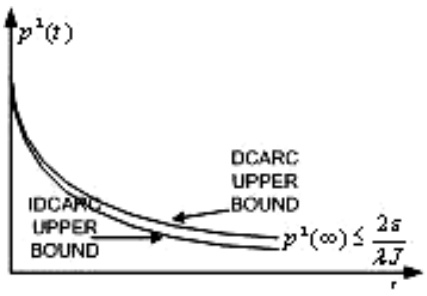

Fig. 5. Upper bound of $p^2(t)$ in ARC and IDCARC

$L_2[\Delta u] = \sqrt{1/N \sum_{j=1}^{N} |u(j\Delta T) - u((j-1)\Delta T)|^2}$ is the normalized control variations.

B. Controller Structures

The following control structures are used in simulations:

• **Mode Switching Control** During the seeking mode of MSC, the servo controller drives the read/write head to follow the desired velocity profile, which is calculated base on a rigid body plant model. Defining the velocity profile as $v(p) = -\text{sgn}(p)\sqrt{2a|p|} - r_t$ if $|p| > 2r_t^2/a$ or $v(p) = -(a/2r_t).p$ if $|p| < 2r_t^2/a$ an approximate time optimal system (PTOS) can be generated [1]. In which, $p, a,$ and r_t are the remaining distance to the target track, the maximum acceleration, and the velocity offset, respectively. In PTOS approach, the back electromotive force, which physically behaves like a linear friction, and the actuator bandwidth, are not taken into consideration and as a result, the velocity profile in PTOS method can only be approximately followed.

• **ARC:** The ARC law proposed in section 3. is applied on the system. With $u_s = -k_s p$, $k_s \geq k_2 + h^2/4\varepsilon$ the control gains are chosen as: $k_1 = 317$ to have a bandwidth about 500 Hz, and $k_s = 1.0$. The adaptation rates are set as $\Gamma = diag\{10,0,1,10000\}$. The initial parameters are chosen as follows:

$\hat{\theta}(0) = [1e-6,\ ,12.5e-6,0,0]^T$ $\theta_{M\alpha} = [0.8e-6, 10e-6, 1e-5, 0.5]^T$

• **DCARC:** The Desired Compensation ARC law with $u_s = -k_s' p$ is applied on the system. The control gains are chosen as $k_s' \geq k_2 + h'^2/4\varepsilon$ to have a bandwidth about 500 Hz $k_1 = 317$ and $k_s' = 1.0$. The adaptation rates are set as $\Gamma = diag\{10,0,1,10000\}$.

• **IDCARC:** The proposed Improved DCARC law is applied on the system. All coefficients are the same as DCARC coefficient and integrator gain in adaptive part is set to $k = 1000$.

C. Simulation Input Signals

In order to have a fair comparison the following sets of simulation input signals are considered:

Set1: To test tracking performance of the controllers in present of friction with A_f =1e-5 as in [3], a 2600 track seeking trajectory is considered in this set, as elaborated in appendix I. and illustrated in Fig. 10.

Set2: A step disturbance input at $t = 10$ msec with amplitude about 0.5mA is considered in this set in addition to the above reference trajectory.

Set3: The performance to the Set 1 reference trajectory in present of %20 variation in system gain is simulated in this set.

D. Controllers Performance

As quantitatively shown in Table II, the simulation result in terms of performance indices e_M and e_F of IDCARC is significantly better than that of ARC and DCARC for all sets, specifically in present of disturbance. As shown in Fig. 6 and 7 it has been observed that ARC is relatively poor to reject disturbance compared to the IDCARC. IDCARC has the best performance in terms of $L_2[u]$, $L_2[e]$, e_M and e_F for all abovementioned sets. The main reason for this significant improvement is due to the proposed dynamic term added in the estimation procedure. It can be seen in the Fig. 6 that the closed loop position results obtained through IDCARC method, has a suitable settling characteristics without any large overshoots and attenuate disturbances extremely better than ARC. It is observed that for larger disturbances ARC becomes unstable but IDCARC can still attenuate disturbances relatively well. In order to analyze the other important issues on the performance of the closed loop system, the control efforts are illustrated in Fig. 7. As it is shown in this figure smooth control effort confirms the advantages of jerk minimized reference input, especially at the time of disturbance enforcement at $t = 10$ msec. Moreover, the low values of obtained errors in the IDCARC method shows the effectiveness of delay compensation. The rejection of the disturbance occurred in $t = 10$ msec in IDCARC method shows superior characteristics in presence of higher

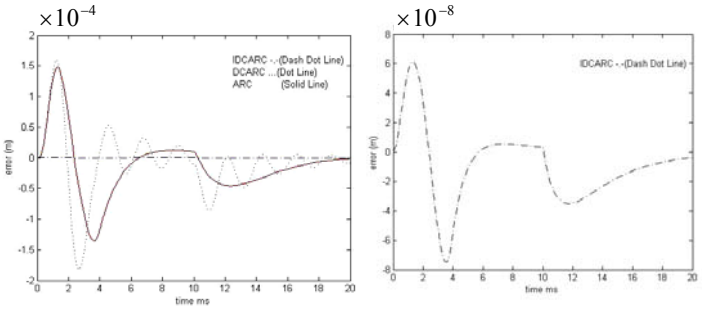

Fig. 6. Tracking error for different methods

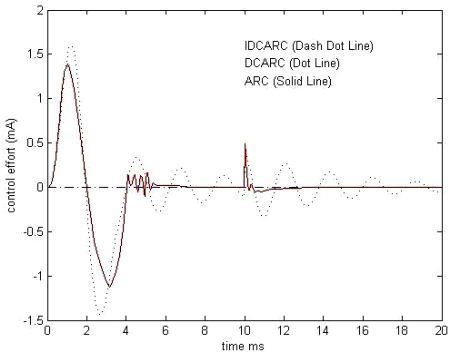

Fig. 7. Control effort for smooth signal generated

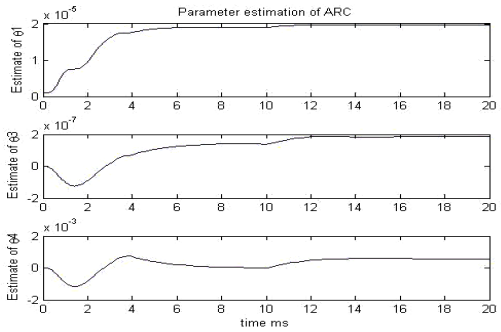

Fig. 8. Parameter estimation of ARC

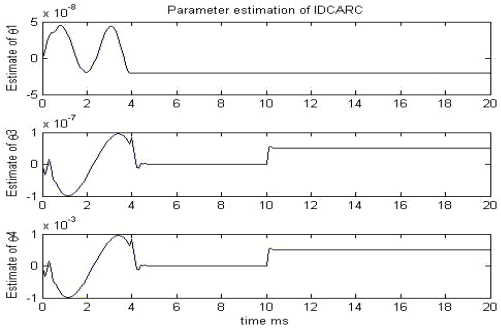

Fig. 9. Parameter estimation of IDCARC

frequency modes considered in the simulated model. Because of the introduced dynamics in adaptation algorithm in IDCARC method, the proposed method is capable to pick up the actual value of disturbance more quickly. This can be seen from the comparison of the parameter estimation rates shown in Figs 8 and 9, in which in the IDCARC method the steady state convergence of the parameters are much faster than that in ARC. Finally, as illustrated in Fig. 10 the track seeking time of IDCARC results are much faster than that in conventional PTOS method.

E. Runout Disturbance and Position Error Signal

The disturbances in a real HDD are usually considered as a lumped disturbance at the plant outputs, known as *runouts*, [16]. Repeatable runouts (RRO) are caused by spindle motor rotation, and consist of frequencies that are multiple spindle frequencies. Non-repeatable runouts (NRRO), on the other hand, are caused mainly due to vibrations and shocks, mechanical disturbance and electrical noise, and hence usually random and unpredictable. Although the effects of the runouts are not considered in our problem formulation, but it turns out that the proposed controller is capable of rejecting the few first modes of the runout disturbances quite effectively. Fig 11 shows the tracking error of ARC and IDCARC controllers, under the simulated disturbance of runouts as in [16]. It is illustrated in this figure how effective is the proposed IDCARC method in runout rejection compared to that to ARC method. In order to have comprehensive performance verification in presence of runout disturbance, the statistical measure of position error signal (PES) can be analyzed. In disk drive applications, the variation of the R/W head from the center of track during track following, which can be directly read off as the PES, is very important. HDD servo system must ensure that PES is kept to a minimum. Having deviations that are above the tolerance of the disk drive would result in too many R/W errors, making the disk drive unusable. A suitable measure is the standard deviation of the readings, σ_{pes}. A useful guideline is to make the $3\sigma_{pes}$ value $<10\%$ of the track pitch, which is about 0.1 μm for a track density of 25kTPI. In the simulations made for the system in hand, the $3\sigma_{pes}$ value for the ARC controller is about 0.0335 μm and for the IDCARC is 1.4238e-5 μm, which shows a significant improvement in terms of disturbance rejection. In case of DCARC the $3\sigma_{pes}$ value is more than 0.1 μm and not acceptable. By this comparison study, the effectiveness of the proposed control algorithm is verified and compared to the other methods.

V. CONCLUSIONS

In this paper, an adaptive robust controller is implemented for hard disk drives (HDD), considering high frequency modes in the model. This method with its unified structure can be applied to both seeking and following modes.

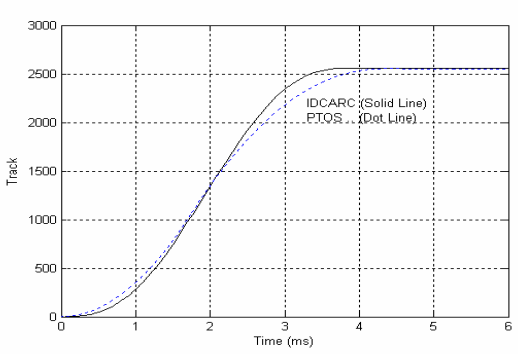

Fig 10. Seeking and following of 2600 tracks

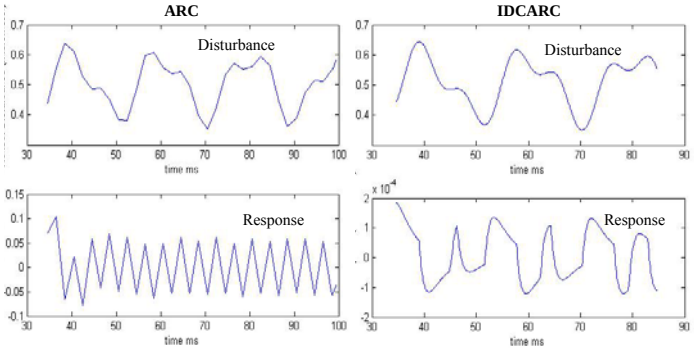

Fig 11. Runout Disturbance and Response in ARC and IDCARC methods

In this proposed method a discontinuous projection based on adaptive robust controller (ARC) is considered first. This controller theoretically guarantees a prescribed transient performance and well behaved tracking in presence of parametric uncertainties. An IDCARC scheme is then proposed, in which the adaptation regressor is calculated using only reference trajectory information. The resulting controller has many implementation advantages. It reduces not only the on-line computation time, but also the induced structural vibration, the effect of the measurement noise, and moreover, it separates the robust control design from parameter adaptation with a faster adaptation rate. A thorough robust analysis of this method is presented first, in which a controller designed based on a simple model of the system is implemented in closed loop on a more comprehensive model for the system. Simulation result verifies the robustness and the significant performance improvement of the IDCARC compared to that of ARC for this model. Moreover, the simulation and comparison results illustrate the ability of the proposed method in achieving suitable control in presence of unstructured model uncertainties, and input disturbances. It is shown

TABLE II
PERFORMANCE INDEX FOR DESIRED TRAJECTORY

Experiments	Set 1			Set 2			Set 3		
Performance Index	ARC	DCARC	IDCARC	ARC	DCARC	IDCARC	ARC	DCARC	IDCARC
$e_M \times 10^{-4}$	1.48	1.82	7.47e-4	1.82	1.48	7.47e-4	1.76	2.78	9.34e-4
$e_F \times 10^{-6}$	0.26	1.21	2.04e-4	8.9	8.45	5.25e-3	7.83	2.2e1	5.19e-3
$L_2[e] \times 10^{-4}$	6.5	7.48	3.2e-3	8.11	6.71	3.83e-3	7.78	13	4.51e-3
$L_2[u] \times 10^{-2}$	0.49	0.66	0.44	0.68	0.50	0.45	0.64	1.10	0.56
$L_2[\Delta u] \times 10^{-4}$	1.05	0.75	0.77	0.84	1.10	0.93	1.39	1.36	1.09
$c_u \times 10^{-2}$	2.15	1.14	1.74	1.25	2.2	2.08	2.17	1.24	1.98

that the IDCARC method is capable of significantly improving the seeking and following performances, and its implementation on a more comprehensive model of the system provides the assurance of its successful experimental implementation.

REFERENCES

[1] G.F. Franklin, J.D. Powell, M. Workman, *Digital control of dynamic systems*, Addison Wesley, 1998.

[2] J.Q. Gong, L. Guo, H. Seong Lee, B. Yao, Modeling and Cancellation of Pivot Nonlinearity in Hard Disk Drive, In Proc. ACC, Anchorage, 2002, 4111-4115.

[3] R. Horowitz, Bo Li, Adaptive track-following servos for disk files servos, In Proc. ACC, 1995, 4161-4166.

[4] S. Hara, T. Hara, Li Yi, M. Tomizuka, Novel reference signal generation for two degree-of-freedom controllers for hard disk drives, IEEE/ASME Trans. on Mechatronics, 5(1), 2000, 73-78.

[5] J. Ishikawa, Y. Yanagita, T. Hattori, M. Hashimoto, Head positioning control for low sampling rate system based on two-degree-of-freedom control, IEEE Trans. Magnetics, 32 (2), 1996, 1787-1792.

[6] Li Yi, M. Tomizuka, Two Degree-of-Freedom control with adaptive robust control for hard disk servo systems, IEEE/ASME Trans. Mecatronics, 4(1), 1999 17-24.

[7] Ben M. Chen, Tong H. Lee, V. Venkataramanan, Composite nonlinear feedback control for linear systems with input saturation theory and application, IEEE Trans. Automatic Control, 48(3), 2003, 427-439.

[8] Q. Hao, R. Chen, G. Guo; S. Chen; T. S. Low, A gradient-based track-following controller optimization for hard disk drive, IEEE Transactions on Industrial Electronics, 50(1), 2003, 108 – 115.

[9] K. Peng, B.M. Chen, G. Cheng, T.H. Lee, Modeling and Compensation of Nonlinearities and Friction in a Micro Hard Disk Drive Servo System With Nonlinear Feedback Control, IEEE Transactions on Control Systems Technology, 13(5) 2005, 708 – 721.

[10] C. Du, L. Xie, J.N. Teoh, G. Guo, An Improved Mixed H2/H∞ Control Design for Hard Disk Drives, IEEE Transactions on Control Systems Technology, 13(5) 2005, 832 – 839.

[11] Li Xu, Bin Yao, Adaptive robust Precision Motion Control of Linear Motors With Negligible Electrical Dynamics: Theory and Experiments, IEEE/ASME Trans. Mechatronics, 6(4), 2001, 444-452.

[12] N. Sadegh, R. Horowitz, Stability and robustness analysis of a class of adaptive controllers for robot manipulators, Int. J. Robot. Res., 9(3), 1990, 74-92.

[13] E. Jamei, H.D. Taghirad, Adaptive robust controller synthesis for hard disk servo systems, In Proc. IEEE/RJS, Conf. on Intelligent Robots and Systems, Sendai, Japan, 2004, 1154-1159.

[14] B. Yao, High performance adaptive robust control of nonlinear systems: A general framework and new schemes, Proc. IEEE Conf. on Decision & Control, San Diego, 1997, 2489-2494.

[15] B. Yao, M. Tomizuka, Smooth robust adaptive sliding mode control of robot manipulators with guaranteed transient performance, Trans. ASME, J. Dyn. Syst., Meas. Cont., 118(4), 1996, 764-775.

[16] V. Venkataramanan, B.M. Chen, T.H. Lee, G. Guo, A new approach to the design of mode switching control in hard disk drive servo systems, Control Engineering Practice, 10(9), Sept. 2002, 925-939.

APPENDIX I: SMOOTH SIGNAL GENERATION METHOD:

To avoid vibration and saturation input signal has been designed based on optimal control. Consider a simple double integrator model for VCM, with the back-emf. For jerk minimization the SMART strategy introduced in [4] is used, in which an optimal control problem for the double integrator plant with the following performance index is considered.

$$J = \int_0^{t_f} \left[\frac{du_{smart}(t)}{dt} \right]^2 dt \tag{35}$$

As illustrated in Fig 12 in this strategy in order to avoid actuator saturation, the maximum motor voltage $u_{\max}$ is used in acceleration and its negative $-u_{\max}$ in deceleration. The acceleration is continued until the motor speed reaches its maximum $v_{\max}$. Then constant speed is kept, until the deceleration mode starts. In order to find the appropriate final time t_f and switching time t_{sw} the optimal problem has been solved analytically, and lookup tables are generated. Simulation results for some discrete switching time k_{sw} are shown in Fig 13, and the values of SMART output, voltage and current is given by the following equations:

$$y_{smart}(k) = (6y_f - 3v_f k_f + \frac{a_f}{2} k_f^{\,2})(k/k_f)^5 + (-15y_f + 7v_f k_f \tag{36}$$
$$-a_f k_f^{\,2})(k/k_f)^4 + (10y_f - 4v_f k_f + \frac{a_f}{2} k_f^{\,2})(k/k_f)^3$$

$$v_{smart}(k) = (30y_f \frac{1}{k_f} - 15v_f + \frac{5a_f}{2} k_f)(k/k_f)^4 + (-60y_f \frac{1}{k_f} + 28v_f \tag{37}$$
$$-4a_f k_f)(k/k_f)^3 + (30y_f \frac{1}{k_f} - 12v_f + \frac{3a_f}{2} k_f)(k/k_f)^2$$

$$i_{smart}(k) = \frac{I_b k_y}{k_T T_s^{\,2}} [(120y_f \frac{1}{k_f^{\,2}} - 60v_f \frac{1}{k_f} + 10a_f)(k/k_f)^3 + (-180y_f \frac{1}{k_f^{\,2}} \tag{38}$$
$$+84v_f \frac{1}{k_f} - 12a_f)(k/k_f)^2 + (60y_f \frac{1}{k_f^{\,2}} - 24v_f \frac{1}{k_f} + 3a_f)(k/k_f)]$$

in which, k is discrete–time index, k_f is final sample number, k_y is one track pitch angle (rad/track), k_T is torque constant, T_s is sampling time(sec), and the current error i_f is converted to an acceleration error using:

$$a_f = i_f \left(k_T T_s^{\,2} \right) / \left(J k_y \right). \tag{39}$$

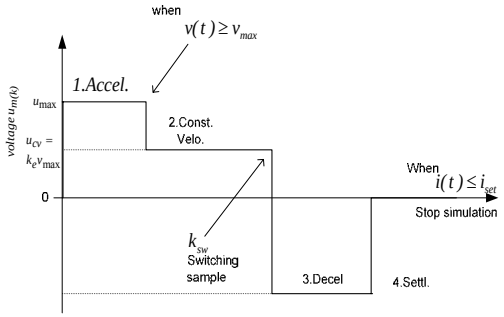

Fig 12. Control input in off-line simulation

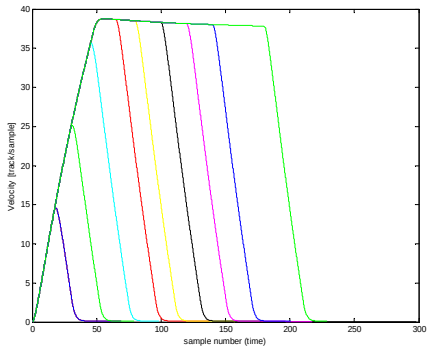

Fig 13. Represented off-line simulation results (head velocity)